UC San Diego

Title
Acute nicotine activates orectic and inhibits anorectic brain regions in rats exposed to chronic nicotine.

Permalink

Authors
Shankar, Kokila
Bonnet-Zahedi, Sélène
Milan, Kristel
et al.

Publication Date

DOI

Peer reviewed

Acute nicotine activates orectic and inhibits anorectic brain regions in rats exposed to chronic nicotine

Kokila Shankar[1], Sélène Bonnet-Zahedi[1,2], Kristel Milan[1], Andrea Ruiz-D'argence[1], Elizabeth Sneddon[1], Ran Qiao[1], Supakorn Chonwattanagul[1], Lieselot Carrette[1], Marsida Kallupi[1], Olivier George[1,*]

[1]Department of Psychiatry, University of California San Diego School of Medicine, La Jolla, CA 92093, USA

[2]Institut de Neurosciences de la Timone, Aix-Marseille Université, Marseille, 13005, France

Abstract

Nicotine use produces psychoactive effects, and chronic use is associated with physiological and psychological symptoms of addiction. However, chronic nicotine use is known to decrease food intake and body weight gain, suggesting that nicotine also affects central metabolic and appetite regulation. We recently showed that acute nicotine self-administration in nicotine-dependent animals produces a short-term increase in food intake, contrary to its long-term decrease of feeding behavior. As feeding behavior is regulated by complex neural signaling mechanisms, this study aimed to test the hypothesis that nicotine intake in animals exposed to chronic nicotine may increase activation of pro-feeding regions and decrease activation of pro-satiety regions to produce the acute increase in feeding behavior. FOS immunohistochemistry revealed that acute nicotine intake in nicotine self-administering animals increased activation of the pro-feeding arcuate and lateral hypothalamic nuclei and decreased activation of the pro-satiety parabrachial nucleus. Regional correlational analysis also showed that acute nicotine changes the functional connectivity of the hunger/satiety network. Further dissection of the role of the arcuate nucleus using electrophysiology found that putative POMC neurons in animals given chronic nicotine exhibited decreased firing following acute nicotine application. These brain-wide central signaling changes may contribute to the acute increase in feeding behavior we see in rats after acute nicotine and provide new areas of focus for studying both nicotine addiction and metabolic regulation.

Keywords

rodent; arcuate; POMC; hypothalamus; self-administration; FOS

*Corresponding author: olgeorge@health.ucsd.edu, 3272 Skaggs Pharmaceutical Sciences Building, 9500 Gilman Dr, La Jolla, CA 92093.

Introduction

Nicotine is consumed for its pleasurable psychoactive effects, including increased arousal, cognition, and mild euphoria caused by activation of dopaminergic neurons[1]. While chronic nicotine use is primarily associated with physiological and psychological symptoms of addiction, it also affects the central regulation of metabolism and feeding behavior. Long-term nicotine use decreases overall food intake, as shown in both human and non-human animal studies[2,3]. Conversely, it is well-established that cessation of nicotine use produces a robust increase in weight gain and self-reported feelings of craving and increased appetite that can contribute to difficulties in quitting nicotine use and ultimately promote relapse[4-7]. However, we recently showed that acute nicotine intake in nicotine-dependent animals produces a short-term increase in feeding behavior – contrary to the overall decrease in feeding seen with long-term nicotine use – suggesting that nicotine may have more complex effects on feeding dysregulation than previously understood[8].

Feeding is a complex behavior, integrating peptidergic and hormonal inputs from the periphery with both homeostatic and hedonic signals in the brain. Together, these signals converge to promote or suppress food intake. Many factors, including energy balance, hormone levels, and even substance use, can alter feeding behaviors. To affect central signaling mechanisms of feeding, peripheral signals interact with the central homeostatic regions of feeding control, the hypothalamus and the nucleus of the solitary tract (NTS)[9,10]. The liaison between the periphery and brain in the hypothalamus is the arcuate nucleus (Arc). There are many different populations of cells in the Arc; the most important players are two distinct neuronal populations that oppositely affect feeding behavior. Agouti-related peptide/neuropeptide Y neurons (AgRP/NPY, referred to from here as AgRP[11]) have been shown in multiple studies to be necessary and sufficient for driving rapid feeding when stimulated[12-14]. Conversely, pro-opiomelanocortin (POMC) neurons inhibit food intake through receipt of leptin signaling and the subsequent activation of the melanocortin system[15-17]. Both neuronal populations receive most of their presynaptic inputs from other hypothalamic nuclei[18]. AgRP and POMC neurons primarily extend reciprocal projections between the arcuate nucleus and other hypothalamic nuclei, including the paraventricular nucleus of the hypothalamus (PVH), lateral hypothalamus (LH), and ventromedial hypothalamus (VMH)[18,19]. The LH receives Arc input to promote food intake[20,21], while the PVH and VMH act as anorexigenic centers to promote satiety[20-23].

As chronic nicotine use dysregulates feeding behaviors and energy metabolism, research has been done to understand how nicotine may affect the above circuitry. Nicotinic acetylcholine receptors (nAChRs) are ubiquitously present in the brain, including the Arc and NTS[24,25]. It has been shown that nicotine activates neurons in both these regions[26,27]. Importantly, Mineur *et al.* showed that nicotine activation of POMC neurons was necessary and sufficient to regulate the decreased feeding associated with chronic nicotine use[28]. However, nicotine also activates AgRP neurons[26], so it is unclear whether this signaling may contribute to the short-term increase in feeding we observed[8]. To identify the possible contribution of central signaling on the acute increase in feeding behavior following nicotine intake in rats given chronic nicotine, we examined both overall changes in regional activation using FOS immunohistochemistry as well as specific changes in Arc neuronal activity using

slice electrophysiology in rats. We hypothesized that nicotine intake in animals chronically exposed to nicotine may increase activation of pro-feeding regions and decrease activation of pro-satiety regions.

Methods

Animals

Adult male and female Wistar rats (N = 26), 8-10 weeks at the start of the study, (Charles River, Hollister, CA, USA) were used for this experiment. All rodents were maintained on a 12/12 h light/dark cycle with *ad libitum* access to food and tap water. All procedures were conducted in strict adherence to the National Institutes of Health guidelines and approved by the University of California San Diego School of Medicine Institutional Animal Care and Use Committee.

Drugs

Nicotine hydrogen tartrate (Glentham, USA) was dissolved in 0.9% sterile saline and pH was adjusted to 7.0. For intravenous nicotine self-administration, animals administered the nicotine solution via indwelling intravenous jugular catheter at a dose of 0.03 mg/kg/infusion (FR1, 20 s timeout). For osmotic minipump delivery, nicotine solution was prepared according to animals' body weight, loaded into osmotic minipumps (Alzet 2ML2, Braintree Scientific, USA) and delivered at a rate of 1 mg/kg/day. Nicotine for application on slices was prepared by making a 1 mM nicotine hydrogen tartrate (Glentham, USA) solution in artificial cerebrospinal fluid (aCSF, recipe in *Experiment 2* procedure below) to achieve a final concentration of 1 μM. Noradrenaline for application on slices was prepared by making a 10 mM noradrenaline bitartrate (Tocris, USA) solution in aCSF to achieve a final concentration of 10 μM.

Experiment 1: Regional FOS activation following acute nicotine intake in nicotine self-administering animals

Male rats (N = 18) were divided into four treatment groups: saline self-administration (SA) and saline injection (Sal/Sal $N = 4$), saline SA and nicotine injection (Sal/Nic, $N = 5$), nicotine SA and saline injection (Nic/Sal $N = 4$) and nicotine SA and nicotine injection (Nic/Nic $N = 5$). These groups were generated to observe the effects of both chronic nicotine intake (Sal/Sal and Nic/Sal) and acute nicotine intake (Sal/Nic and Nic/Nic) on regional cellular activation.

Intravenous jugular catheter implantation was performed according to established lab protocol[8,29]. Briefly, all animals were anesthetized using an isoflurane/oxygen vapor mixture (1-5%). The rats had an intravenous catheter implanted into their right jugular veins, and this catheter was connected to an external port on the middle of the back. Animals were allowed to recover for 5-7 days, during which time catheters were flushed daily with 0.1 mL of sterile physiological saline containing heparin (30 USP units/mL) and the antibiotic cefazolin. Animals were also flushed with this mixture prior to the start of each operant session. After recovery, catheter patency was tested with the ultra-short-acting barbiturate

Brevital sodium. Animals were flushed with 0.1 mL Brevital, and rats with patent catheters exhibited pronounced loss of muscle tone within seconds of the intravenous injection.

All experiments were conducted at the beginning of the dark cycle in sound-attenuating operant conditioning boxes (MedAssociates, Inc., St. Albans, VT, USA). Animals were first trained to self-administer for food (45mg grain-based pellets, TestDiet, USA) and tap water on a fixed-ratio 1 (FR1) schedule in 21 h sessions with no timeout and no access to nicotine lever. Animals were trained for a total of 7-10 days before and after catheter implantation or until a stable baseline intake (±10%) was reached. Animals were not given access to the active or inactive levers during this period.

The active and inactive levers were then presented, and animals first underwent a short access (ShA, 1 h/day) paradigm for 5 days to train for lever pressing. The active lever activated a cue light and delivered the nicotine solution at 0.03 mg/kg/100 μL/1 s (free base, fixed-ratio 1 [FR1], time-out [TO] 20s), while the inactive lever did not produce any response. Next, animals were given continuous long access (LgA, 21 h/days) to the active and inactive levers for 7 days to establish baseline intake. Finally, the animals were transitioned to an intermittent extended access paradigm (IntA) (4 days of 21 h/day access (ON), 3 days without access (OFF)) for 2 weeks to escalate nicotine intake. A control group followed this protocol but intravenously self-administered 0.9% saline. During all of these sessions, animals had *ad libitum* operant access to food and water on the same FR1 schedule.

After the IntA period, animals underwent one additional ON session with access to the active lever, inactive lever, food lever, and water nosepoke. At the end of this session, rats were administered via the MedPC program either three acute intravenous infusions of nicotine (0.09 mg/kg/300 μL/3 s, Sal/Nic and Nic/Nic) or three acute intravenous infusions of 0.9% saline (Sal/Sal and Nic/Sal). This dose was chosen as it best mimics the 'burst' of drug-taking that animals tend to self-administer, enabling us to better capture the reinforcing effects of nicotine and also better replicate the conditions under which we observed the increased feeding behavior[8]. Animals were sacrificed via CO_2 asphyxiation 90 min following infusion in order to allow for expression of FOS protein resulting from neuronal activation. Brains were harvested and immediately transferred to 4% paraformaldehyde (PFA) to begin the post-fixation process for immunohistochemical analyses. Brains were kept in 4% PFA at 4°C for 1 week, changing solution every 1-2 days, and were then transferred to a cryoprotective solution of 30% sucrose with 0.1% sodium azide and kept at 4°C until use.

40 μm sections were sliced from brains at −15 to −20°C on a cryostat (Leica CM1950), and sections were kept in a solution of 1X PBS with 0.1% sodium azide until use. Sections containing the following regions were mounted onto microscope slides in preparation for FOS immunohistochemistry: arcuate nucleus, lateral hypothalamus, paraventricular nucleus, ventromedial hypothalamus, nucleus of the solitary tract, lateral parabrachial nucleus, habenula (lateral + medial), interpeduncular nucleus.

The slides were first incubated in citric acid (0.01 M in MilliQ purified water (mH$_2$O) at pH 6) for 16 minutes at 80-95°C using a microwave oven in order to unmask antigens which become cross-linked with formalin during the post-fixation process. The slides were rinsed in 1X PBS before incubation in 0.3% H$_2$O$_2$ for 30 minutes to quench endogenous peroxidases. Then, the samples were rinsed in 1X PBS, and slices were outlined with a PAP pen (ImmEdge Pen #H-4000) to minimize reagent volume. Blocking was performed using 5% normal goat serum and 0.5% Triton-x100 in 1X PBS at RT for 60 minutes. Primary antibody (c-FOS Rabbit Monoclonal #2250, Cell Signeling Technologies) was diluted 1:1000 in 1X PBS with 0.5% Tween-20 and 5% normal goat serum and immediately applied to slices following blocking, and samples were left to incubate overnight at RT. Following primary incubation, slices were washed with 1X PBS and incubated with an undiluted ready-to-use biotinylated goat anti-rabbit IgG secondary antibody (Vector Laboratories) for 30 minutes. Slices were washed in 1X PBS and Avidin-Biotin Complex (Vectastain Elite ABC-HRP Kit, Vector Laboratories) was applied to the slices for 60 minutes. Slices were visualized using a DAB substrate kit (DAB Substrate Kit, Peroxidase with Nickel, Vector Laboratories). Slices were then dehydrated in 95% ethanol, 100% ethanol, and Citrisolv (d-limonene) in preparation for cover slipping and imaging. DPX (Sigma) was used to mount coverslips, and slices were dried for 48 h before imaging.

Slides were imaged in brightfield at 10X magnification using an inverted fluorescence phase contrast microscope (Keyence BZ-X810). Image files were saved as .tif for analysis. Raw files were cropped to focus on brain regions of interest in Fiji (ImageJ) freeware. Using the Paxinos and Watson rat brain atlas, an outline of the brain region was carefully drawn and only cells within that drawing were counted. For all regions examined in this study, slices were taken from approximately the same antero-posterior location in the brain to minimize variability in neuronal activation across the region. Neuronal activation within each brain region of interest was measured as the number of cells counted manually per mm^2 of the brain region drawn according to the Paxinos and Watson rat brain atlas (Supplementary Fig. 1).

Experiment 2: AgRP and POMC neuronal firing following nicotine application in nicotine-exposed animals

Male and female animals (N = 6 M, 4 F) were subcutaneously implanted with a minipump containing either 1 mg/kg/day nicotine (N = 3 M, 2 F), or 0.9% saline (N = 3 M, 2 F). Minipump implantation surgery was performed by first anesthetizing animals using isoflurane, and then a small incision was made along the middle of the back. The subcutaneous space was opened via blunt dissection, the minipump was carefully inserted, and the wound was sealed using wound clips and skin glue to ensure the pump did not fall out. All animals received the antibiotic cefazolin and the analgesic flunixin (2.5 mg/kg) post-operatively. Animals maintained nicotine minipumps on board for 2 weeks to establish chronic nicotine exposure[30], and animals were sacrificed with minipumps on board to avoid spontaneous withdrawal.

Animals were deeply anesthetized with isoflurane, and brains were quickly extracted and transferred to ice-cold oxygenated (95% O$_2$, 5% CO$_2$) solution containing 206 mM sucrose,

2.5 mM KCl, 1.2 mM NaH$_2$PO$_4$, 7 mM MgCl$_2$, 0.5 mM CaCl$_2$, 26 mM NaHCO$_3$, 5 mM glucose, and 5 mM Hepes. Transverse slices (300 μm) containing the arcuate nucleus were cut on a Vibratome (Leica VT1200S; Leica Microsystems) and transferred to oxygenated artificial cerebrospinal fluid (aCSF) that contained 130 mM NaCl, 2.5 mM KCl, 1.2 mM NaH$_2$PO$_4$, 2.0 mM MgSO$_4$·7H$_2$O, 2.0 mM CaCl$_2$, 26 mM NaHCO$_3$, and 10 mM glucose. The slices were first incubated for 30 min at 35 °C and then kept at room temperature for the remainder of the experiment. Individual slices were transferred to a recording chamber that was mounted on the stage of an upright microscope (Olympus BX50WI). The slices were continuously perfused with oxygenated aCSF at a rate of 2 to 3 mL/min. Neurons were visualized using a 60× water-immersion objective (Olympus BX50WI), infrared differential interference contrast optics, and a charge-coupled device camera (EXi Blue; QImaging). Whole-cell recordings were performed using a Multiclamp 700B amplifier (10-kHz sampling rate, 10-kHz low-pass filter) and Digidata 1440A and pClamp 10 software (Molecular Devices). Patch pipettes (4–7 MΩ) were pulled from 100 ± 3 mm long borosilicate glass with ID: 1.16 +/_0.05 mm and OD: 1.5+/− 0.05 mm with inner diameter 1.16 ± 0.05 mm and outer diameter 1.5 ± 0.05 mm (King Precision Glass, Inc.)) and filled with an internal solution containing 70 mM KMeSO$_4$, 55 mM KCl, 10 mM NaCl, 2 mM MgCl$_2$, 3 mM Mg$_2$, 10 mM Hepes, 3 mM Mg$_2$ Na-ATP, and 0.3 mM Na$_3$-GTP. Liquid junction potential corrections were performed offline. Using the current-clamp method, baseline recording of the firing rate (spikes/second) was taken for 5-10 minutes. 1 μM nicotine (free base) was then applied to the bath and firing rate was recorded for another 5-10 minutes post-application. After a washout period, 10 μM noradrenaline (noradrenaline bitartrate, Tocris) was applied to the bath. Noradrenaline was used to putatively classify cells as AgRP or POMC, as it significantly and oppositely alters firing of these neuronal types[31]. An increase in firing following noradrenaline is specific to AgRP neurons, while a decrease in firing is specific to POMC neurons. Noradrenaline is applied after the nicotine treatment to prevent any confounding effects on cell firing after nicotine, so cells cannot be putatively classified prior to recording. The frequency of the action potentials was analyzed using semiautomated threshold-based mini detection software (Easy Electrophysiology) and visually confirmed.

Statistics

Self-administration data were analyzed by mixed model analysis with Tukey's multiple comparisons *post hoc*. FOS data are expressed as cells/mm^2 of each slice. To account for the variance caused by individual slices within each animal (N = 4-5 animals per treatment group, 2-6 slices per animal), data were analyzed using a linear mixed model (Type III ANOVA) in IBM SPSS 28. *Post hoc* pairwise comparisons were conducted between treatment groups of interest using Student's *t*-test with Holm-Bonferroni correction for multiple comparisons[32] if the interaction of the mixed model effects was significant. Correlational heatmaps were created by combining average cells/mm^2 of each slice for each animal receiving either acute saline injection (N = 8) or acute nicotine injection (N = 10). Pearson's correlational analysis was used to calculate correlations of activation between each brain region, and hierarchical clustering was performed in R to organize brain regions. Electrophysiology data were analyzed using either *t*-tests (percent change from baseline) or 2-way ANOVA with Sidak's multiple comparisons *post hoc* (firing rate).

Results

Nicotine increases activity in the habenular-interpeduncular nucleus circuit

We first examined the effects of a history of nicotine self-administration (SA) and acute nicotine infusion (0.09 mg/kg/300 μL) on the habenula and interpeduncular nucleus (IPN), following confirmation of the self-administration paradigm in eliciting escalation of nicotine intake (main effect of SA $F_{(1,18)} = 4.600$, $p = 0.0459$; Supplementary Fig. 2). Both regions are densely populated with nicotinic acetylcholine receptors, and the habenula-IPN axis plays a critical role in mediating nicotine intake and withdrawal[33,34]. We hypothesized that acute infusion of nicotine would increase activation of these regions, and nicotine self-administration may not yield significant activation due to nicotine receptor desensitization associated with chronic use. Both chronic nicotine and acute infusion significantly increased activation of the habenula (main effect of SA $F_{(1,85)} = 46.22$, $p < 0.001$; main effect of infusion $F_{(1,85)} = 134.4$, $p < 0.001$) (Fig. 1A). However, there was no significant effect of the interaction between the two variables. In the IPN, we observed a significant increase in activation following acute infusion of nicotine (main effect of infusion $F_{(1,43)} = 11.02$, $p = 0.002$) (Fig. 1B). Our data suggests that nicotine self-administration and acute nicotine infusion both increase activation of the habenular-IPN circuit.

Nicotine increases the activity of pro-feeding arcuate and lateral hypothalamic nuclei.

As we are interested in identifying central signaling changes that may contribute to the increased feeding behavior following acute nicotine infusion in animals chronically self-administering nicotine, we next examined the activation of key hypothalamic nuclei known to promote feeding. We hypothesized that nicotine infusion in nicotine self-administering animals would significantly increase activation in these regions. Mixed model analysis across treatment groups showed that the Arc exhibited significantly increased activation in nicotine-self-administering animals following acute nicotine treatment compared with saline self-administering animals (SA × infusion interaction $F_{(1,53)} = 15.19$, $p < 0.001$; main effect of SA $F_{(1,53)} = 13.87$, $p < 0.001$) (Fig. 2A). *Post hoc* analysis using Student's *t*-test revealed that Nic/Nic animals had significantly more activation compared with Nic/Sal and Sal/Nic animals ($p = 0.0002$ and $p < 0.0001$, respectively).

Using mixed model analysis to compare activation in the lateral hypothalamus (LH) across treatment groups, we found that both nicotine self-administration and acute infusion of nicotine significantly increased FOS activation (main effect of SA $F_{(1,95)} = 73.21$, $p < 0.001$; main effect of infusion $F_{(1,95)} = 20.72$, $p < 0.001$) (Fig. 2B). Specifically, acute nicotine infusion significantly increased LH activation in nicotine self-administering animals (SA × infusion interaction $F_{(1,95)} = 11.47$, $p = 0.001$). Student's *t*-test *post hoc* revealed that the Nic/Nic group exhibited significantly more FOS activation than the Nic/Sal and Sal/Nic groups ($p < 0.0001$ for both). Additionally, the Nic/Sal group had significantly higher activation compared with the Sal/Sal group ($p < 0.0001$) Sal/Nic groups. Therefore, the data shows that pro-feeding hypothalamic nuclei are significantly activated following nicotine infusion in nicotine self-administering animals.

Nicotine exerts mixed effects on activity of anorexigenic hypothalamic and hindbrain nuclei.

We conversely hypothesized that increased feeding behavior could be related to decreased activation of anorexigenic centers within the brain. Within the hypothalamus, we examined both the paraventricular nucleus (PVH) and the ventromedial nucleus (VMH). In the PVH, both nicotine self-administration and acute nicotine treatment significantly altered FOS activation (SA × infusion interaction $F_{(1,52)} = 9.504$, $p = 0.003$,) (Fig. 3A). Specifically, Student's t-test *post hoc* revealed that Sal/Nic animals had significantly decreased activation compared to Sal/Sal animals (Sal/Nic *vs.* Sal/Sal $p = 0.0015$). In slices from the VMH, both nicotine self-administration and acute nicotine infusion increased neuronal activation (main effect of SA $F_{(1,94)} = 5.805$, $p = 0.018$; main effect of infusion $F_{(1,94)} = 5.244$, $p = 0.024$) (Fig. 3B).

In the hindbrain, the solitary tract nucleus (NTS) is the primary liaison and integrator of peripheral signals with downstream central signaling. Nicotine self-administration significantly increased NTS activation (main effect of SA $F_{(1,77)} = 4.029$, $p = 0.048$) (Fig. 3C). However, we did not observe a significant effect of acute nicotine infusion on FOS activation across treatment groups in this region. The lateral parabrachial nucleus (LPBN) is the key anorexigenic nucleus receiving inputs from the NTS. Nicotine-self-administering animals receiving acute nicotine had significantly decreased activation of the LPBN compared to other treatment groups (SA × infusion interaction $p < 0.001$, $F_{(1,78)} = 20.30$) (Fig. 3D). *Post hoc* analysis using Student's t-test revealed that Nic/Nic had significantly decreased activation compared to both Sal/Nic and Nic/Sal animals ($p = 0.0067$ and $p = 0.0012$, respectively). Sal/Nic animals and Nic/Sal animals had significantly increased activation compared with Sal/Sal animals ($p = 0.0009$ and $p = 0.001$, respectively). These data show that anorexigenic nuclei exhibit a mixed response to nicotine, with decreased activation of the LPBN following acute nicotine infusion in animals chronically self-administering nicotine.

Acute nicotine injection increases regional co-activation.

As we found significant differences in FOS expression across treatment groups within multiple regions, we sought to examine how these regions changed in relation to each other. Specifically, we chose to examine the effect of acute nicotine injection on the regional network through the use of functional connectivity – *i.e.*, "cells that fire together, wire together". Functional connectivity examines patterns of neuronal co-reactivity to determine larger patterns of synchronous firing that can represent changes in brain states. Correlational analysis with hierarchical clustering of brain regions revealed significant negative correlations between the VMH and NTS (R = –0.799, $p = 0.031$) and the VMH and IPN (R = –0.833, $p = 0.031$) following acute saline injection, but not following acute nicotine injection (Fig. 4A). Following acute nicotine injection, the habenula was significantly positively correlated with the Arc (R = 0.828, $p = 0.006$) and the LH (R = 0.743, $p = 0.022$) (Fig. 4B). The Arc and LH were also significantly positively correlated with each other (R = 0.728, $p = 0.017$). There was also a significant correlation between the NTS and IPN (R = 0.778, $p = 0.023$). These results suggest that acute nicotine injection

changes the functional connectivity of the hunger/satiety network and increases co-activation between the habenula and two key regions for hunger, the Arc and LH.

Nicotine application alters the firing of arcuate nucleus neurons.

As we observed a significant increase in activation of the Arc following acute nicotine infusion in nicotine-self-administering animals, we wanted to examine changes in cellular signaling in this region. The Arc has two distinct neuronal populations, AgRP and POMC neurons, that exert opposing effects on feeding and are both activated by nicotine. To measure activity within rat brain slices, we used an electrophysiology protocol that relies on applying noradrenaline to the cell post-nicotine application to putatively identify the cell as putative POMC neurons, based on a study by Paeger *et al.* which found that noradrenaline specifically decreases POMC neuron firing[31]. We hypothesized that putative nicotine application would decrease firing of putative POMC neurons.

Brains were collected from animals implanted with either a minipump containing 1 mg/kg/day nicotine (nicotine group) or 0.9% saline (vehicle group) for 2 weeks, and neurons from the Arc were patched (Fig. 5A-B). All vehicle and nicotine cells that were patched exhibited significantly decreased firing following noradrenaline application ($p = 0.0281$, $t = 2.615$, paired *t*-test) (Fig. 5C). Thus, we putatively identified these cells as POMC neurons. In vehicle cells, nicotine application increased firing compared to baseline, while in cells from chronic nicotine animals, nicotine application significantly decreased firing compared to baseline ($p < 0.0001$, $t = 8.477$, Student's t-test) (Fig. 5D-F). Analysis of acute nicotine application by repeated-measures 2-way ANOVA with Sidak's multiple comparisons *post hoc* revealed that the firing rate in nicotine cells was significantly decreased following nicotine application, while vehicle cells' firing was significantly increased after nicotine application (main effect of chronic nicotine $F_{(1,16)} = 17.53$, $p = 0.0031$, chronic nicotine $\times$ treatment interaction $F_{(1,16)} = 31.21$, $p < 0.0001$) (Fig. 5F). This finding demonstrates that acute nicotine application leads to a decrease in the firing of putative POMC neurons in animals with chronic nicotine exposure.

Discussion

The goal of this study was to determine whether acute nicotine would increase activation of pro-feeding-related signaling in the brain and decrease activation of pro-satiety-related signaling, potentially relating to the acute increase in feeding behavior we previously observed. We found that nicotine self-administration and acute nicotine intake increased FOS activation of the habenular-IPN axis. We also found that nicotine significantly increased activation within the Arc and LH. In the hindbrain, we found that LPBN activity increased with nicotine self-administration, but acute infusion of nicotine significantly decreased activation in these animals. We also identified using correlational analysis the co-activation of the habenula, Arc, and LH following acute nicotine injection. Electrophysiological study of the Arc revealed a decrease in POMC firing following nicotine application in animals chronically exposed to nicotine. These results suggest that acute nicotine intake activates pro-feeding circuitry and decreases anorexigenic activity in the brain inchronically nicotine-exposed rats.

Both nicotine self-administration and acute nicotine infusion significantly increased FOS expression in the habenula, and acute nicotine infusion significantly increased IPN activation. These results align with previous studies, as the habenula-IPN circuit is known to be critical for modulating the rewarding and aversive effects of nicotine and nicotine withdrawal[33,34]. The habenula has both lateral and medial components that control different components of nicotine addiction. The lateral habenula is connected to reward processing, whereas the medial habenula is more important for the withdrawal and aversive-like effects of nicotine[35,36]. The medial habenula projects to the IPN, and repeated exposure to nicotine sensitizes this circuit and increases excitability of IPN neurons[37]. We studied the habenula-IPN axis as a validation of the effects of nicotine, and thus did not distinguish lateral *vs.* medial in our analysis; however, future experiments that explore the relationship between the homeostatic and hedonic components of nicotine-induced feeding behavior can further tease apart each subregion's contribution. Interestingly, the medial habenula has been shown to be impacted by metabolic inputs. Circulating glucose alters habenular cholinergic transcription, and GLP-1 activates the medial habenula-IPN circuit and decreases nicotine intake[38,39].

Our correlational analysis also showed significant correlation between habenular activation and Arc and LH nuclei, suggesting that these regions are functionally connected. Functional connectomics, pioneered for the visualization of fear networks in mice, derives a network for a specific brain state or following a specific stimulus based on the correlation in FOS expression between brain regions across the subjects [72, 73]. This method is similar to the time-based correlation analysis of blood oxygenation levels as a measure of neuronal activity in functional MRI (BOLD fMRI) because it does not measure or assume actual structural connections but instead functionally relates regions that exhibit increased activation. This technique has since been used by our lab and others to visualize the functional connectome associated with addiction-related brain changes, including the development of dependency, the 3-stage framework of addiction, and the dual organization of the brain cholinergic system [74-78]. The increased correlation of nicotine addiction-related regional activation (habenula) and feeding-related regional activation (Arc, LH) presented in this report suggests that acute nicotine alters the functional connectivity of the hunger/satiety network, which may play a role in producing a transient increased feeding behavior following acute nicotine intake. Other studies have demonstrated structural connections between the habenula and LH in regulating the emotional valence of food intake [79], further reinforcing a link between this region and its role in feeding.

Both nicotine self-administration and acute nicotine infusion significantly increased activation of cells within the Arc and the LH. These regions are critical for driving feeding, and these results align with our hypothesis that acute nicotine infusion in animals chronically self-administering nicotine would activate pro-feeding regions. The correlational analysis showed a significant positive correlation in activation of these two regions. Previous studies have shown that the Arc projects to the LH, and stimulation of this region increases feeding behavior[18,20]. A general limitation of our immunohistochemical analyses is the inability to further distinguish cell types activated following nicotine infusion. Additional experiments, such as co-staining for AgRP and/or POMC in the Arc, may help better understand the effect of nicotine on specific neuronal populations.

Contrary to our expectations, we did not observe significant decreases in activation of the PVH or VMH, strong anorexigenic regions within the hypothalamus. In fact, in the PVH, we saw that nicotine self-administration significantly decreased activation in Sal/Nic and Nic/Sal animals, but not in Nic/Nic animals as we expected. This region is known to be regulated by the melanocortin system, the neuropeptide signaling system critical for POMC neuron function and general suppression of food intake[41]. However, the PVH contains a heterogeneous population of neuronal subtypes, and is not only activated by nicotine, but also receives input from multiple regions including the Arc, NTS, and LPBN[42-45]. Consequently, the PVH is more appropriately thought of as an integrator of signals within the hypothalamus. Further characterization of the cell types being activated within this region is necessary to better understand these results. We also did not see a significant effect of acute injection of nicotine on NTS activation. Interestingly, the data points within Nic/Nic group appear to have a bimodal distribution where half the animals exhibit higher activation and half exhibit lower activation. While the NTS is believed to regulate satiety, it does contain mixed orexigenic/anorexigenic inputs[46,47]. Thus, the split in data could reflect both a decrease in anorexigenic signaling and an increase in orexigenic signaling. Again, further immunohistochemical analysis is required to fully tease out the signaling changes that are occurring.

LPBN activation significantly increased in Sal/Nic and Nic/Sal groups, but significantly decreased in Nic/Nic animals. The LPBN is a critical anorexigenic region in the hindbrain[48], and these results match our hypothesis that while nicotine elicits increased anorexigenic signaling with long-term use, acute nicotine intake in these animals conversely decreases it. While we did not observe any significant correlations with LPBN activity in our network analysis, studies have shown that AgRP projections to the LPBN can inhibit its activity[48-50]. As we saw increased signaling within the Arc, this connection may contribute to the results.

Within the Arc, both the AgRP and POMC neurons play a critical role in regulating feeding. We observed that chronic nicotine increased baseline firing of putative POMC neurons, but acute nicotine application in nicotine-exposed rats significantly decreased putative POMC neuron firing. These results confirm our initial hypothesis that acute nicotine application in animals chronically exposed to nicotine would decrease firing of satiety-regulating cells in the Arc. A seminal study by Mineur *et al.* found that chronic nicotine administration decreased food intake in mice and increased firing of POMC neurons as measured by FOS reactivity[28]. Our data corroborate this finding as we demonstrated increased baseline firing in POMC neurons following chronic nicotine. Mineur *et al.* further observed an increase in POMC firing following acute application of nicotine in naïve animals. Conversely, we found that putative POMC firing increased following nicotine application in vehicle-treated animals, but putative POMC firing decreased following nicotine application in nicotine-exposed animals. These opposing effects of nicotine on firing can possibly help explain the behavioral phenomenon that acute nicotine intake in dependent animals produces acute increased food intake while chronic nicotine decreases food intake. POMC neurons have GABAergic efferents from AgRP neurons; as AgRP neurons are stimulated, they then inhibit the firing of POMC neurons[19]. Synthesizing our electrophysiology findings with the increased Arc activation we observed, this may contribute to the mechanism through which

we see the increased feeding behavior. However, analysis of AgRP neurons is required to determine whether nicotine application produces increased firing of these cells.

The current study utilized FOS immunohistochemistry to study regional activation as FOS, the product of immediate-early gene *c-fos* expression, is a well-established marker of neuronal reactivity and is upregulated by nicotinic stimulation of neurons[51,52]. The majority of studies examining FOS changes in response to acute nicotine have previously used high doses (0.5 – 2 mg/kg)[53,54] known to often produce aversion[30], and these doses may not be relevant to the acute anti-anorectic effect of nicotine self-administration which is observed with both self-administration and passive experimenter administration of lower doses (0.06-0.09 mg/kg)[8]. As this behavior is a nicotine-specific effect that is not only a consequence of self-administration or operant behavior, we chose to use passive administration of nicotine to avoid variability in animal self-administration. In this study, we used low doses of nicotine (0.09 mg/kg/300 μL intravenous infusion, 1 μM slice application) to better approximate the low dose that rats self-administer in order to identify neuronal populations that may be mediating the anti-anorectic effect of self-administered nicotine.

A limitation of the current study is the use of noradrenaline to putatively identify cells as POMC neurons. A study by Paeger *et al.* found that noradrenaline differentially modulates AgRP and POMC neurons, where AgRP exhibit significantly increased firing and POMC neurons exhibit significantly decreased firing after noradrenaline application[31]. As noradrenaline produces completely opposite responses in these two cell types, and as these two cell types are the primary populations within the Arc, this approach was valuable in helping identify these neurons without employing a transgenic fluorescent reporter model. We applied this treatment after nicotine to avoid confounding effects on firing after nicotine application. Because there are no obvious morphological differences between AgRP and POMC neurons[19], it can be difficult to distinguish the neuron type prior to recording. We opted to use this approach as it allowed us to continue our rat model in which we have validated the increased feeding behavior[55]. Commercially available mouse models exist that fluorescently label POMC and AgRP neurons (Jackson Laboratories), but these would require extensive behavioral validation. Few viral vectors exist to target rat AgRP or POMC cells, and they often have poor specificity[56]. Future studies employing labeling methods to characterize AgRP *vs.* POMC neurons in rat brain slices are necessary to confirm the effect of acute nicotine application on these cells.

Finally, while we focused on examining the activation of regions primarily known to mediate food intake, an important consideration is the role these regions play in other behaviors. Tbe hypothalamic nuclei we examined are necessary for other homeostatic functions such as cardiovascular regulation, sleep, arousal, and thermogenesis[57-62]. Interestingly, both the paraventricular hypothalamus and lateral parabrachial nucleus have reciprocal projections to the central amygdala, and these connections are known to be involved in stress response, fear acquisition, and pain[63-65]. Chronic nicotine has been shown to increase brown adipose tissue thermogenesis, increase signaling of corticotropin-releasing factor and the hypothalamic-pituitary-adrenal axis, and worsen sleep[66-68]. While it is currently unclear whether changes to these homeostatic mechanisms contribute to increased

feeding following acute nicotine, further studies are needed to decipher the FOS expression of cells regulating feeding behavior *vs.* other homeostatic behaviors.

It is also essential to understand how hedonic circuitry may contribute to nicotine-induced changes in feeding behaviors[69]. Beyond the habenular-IPN circuit, many of the regions we analyzed have inputs from and outputs to regions involved in the addiction cycle[70]. Additionally, dopamine release in the nucleus accumbens can be stimulated by both nicotine and food intake[71], implicating the ventral tegmental area in feeding-related circuitry as well as the rewarding effects of nicotine. Further analysis of the activation of addiction-related brain regions, including the ventral tegmental area, nucleus accumbens, amygdala, insular cortex, and striatum, as well as the correlation between activation of those regions and feeding-related regions would be necessary to deduce whether the acute increase in feeding behavior is driven through physiological or psychological changes following the establishment of nicotine dependence.

In summary, this study focused on the effects of both chronic nicotine exposure and acute nicotine intake on regional and cellular signaling in the brain. We found that acute nicotine in animals chronically exposed to nicotine increases activation of pro-feeding neurons and decreases activity of anorexigenic neurons. These brain-wide network modulations may contribute to the acute increase in feeding behavior we see in rats after acute nicotine and provide new areas of focus for studying both nicotine addiction and metabolic regulation.

Supplementary Material

Refer to Web version on PubMed Central for supplementary material.

Funding

References

1. Benowitz NL Nicotine Addiction. New England Journal of Medicine 362, 2295–2303 (2010). [PubMed: 20554984]

2. Bellinger LL, Wellman PJ, Harris RBS, Kelso EW & Kramer PR The effects of chronic nicotine on meal patterns, food intake, metabolism and body weight of male rats. Pharmacology Biochemistry and Behavior 95, 92–99 (2010). [PubMed: 20035781]

3. Audrain-McGovern J & Benowitz NL Cigarette Smoking, Nicotine, and Body Weight. Clinical Pharmacology & Therapeutics 90, 164–168 (2011). [PubMed: 21633341]

4. Aubin H-J, Farley A, Lycett D, Lahmek P & Aveyard P Weight gain in smokers after quitting cigarettes: meta-analysis. BMJ 345, e4439 (2012). [PubMed: 22782848]

5. Filozof C, Pinilla MCF & Fernández-Cruz A Smoking cessation and weight gain. Obesity Reviews 5, 95–103 (2004). [PubMed: 15086863]

6. Harris KK, Zopey M & Friedman TC Metabolic effects of smoking cessation. Nat Rev Endocrinol 12, 299–308 (2016). [PubMed: 26939981]

7. Perkins KA Weight Gain Following Smoking Cessation. 10.

8. Shankar K, Ambroggi F & George O Microstructural meal pattern analysis reveals a paradoxical acute increase in food intake after nicotine despite its long-term anorexigenic effects. Psychopharmacology 239, 807–818 (2022). [PubMed: 35129671]

9. Rui L. Brain Regulation of energy balance and body weights. Rev Endocr Metab Disord 14, (2013).

10. Ahima RS & Antwi DA Brain regulation of appetite and satiety. Endocrinol Metab Clin North Am 37, 811–823 (2008). [PubMed: 19026933]

11. Hahn TM, Breininger JF, Baskin DG & Schwartz MW Coexpression of Agrp and NPY in fasting-activated hypothalamic neurons. Nat Neurosci 1, 271–272 (1998). [PubMed: 10195157]

12. Atasoy D, Betley JN, Su HH & Sternson SM Deconstruction of a neural circuit for hunger. Nature 488, 172–177 (2012). [PubMed: 22801496]

13. Aponte Y, Atasoy D & Sternson SM AGRP neurons are sufficient to orchestrate feeding behavior rapidly and without training. Nature Neuroscience 14, 351–355 (2011). [PubMed: 21209617]

14. Chen Y. et al. Sustained NPY signaling enables AgRP neurons to drive feeding. eLife 8,.

15. Cowley MA et al. Leptin activates anorexigenic POMC neurons through a neural network in the arcuate nucleus. Nature 411, 480–484 (2001). [PubMed: 11373681]

16. Zhan C. et al. Acute and Long-Term Suppression of Feeding Behavior by POMC Neurons in the Brainstem and Hypothalamus, Respectively. J. Neurosci 33, 3624–3632 (2013). [PubMed: 23426689]

17. Millington GW The role of proopiomelanocortin (POMC) neurones in feeding behaviour. Nutrition & Metabolism 4, 18 (2007). [PubMed: 17764572]

18. Wang D. et al. Whole-brain mapping of the direct inputs and axonal projections of POMC and AgRP neurons. Front. Neuroanat 9, (2015).

19. Sohn J-W Network of hypothalamic neurons that control appetite. BMB Rep 48, 229–233 (2015). [PubMed: 25560696]

20. Delgado JMR & Anand BK Increase of Food Intake Induced by Electrical Stimulation of the Lateral Hypothalamus. American Journal of Physiology-Legacy Content 172, 162–168 (1952).

21. Qualls-Creekmore E & Münzberg H Modulation of Feeding and Associated Behaviors by Lateral Hypothalamic Circuits. Endocrinology 159, 3631–3642 (2018). [PubMed: 30215694]

22. Li MM et al. The Paraventricular Hypothalamus Regulates Satiety and Prevents Obesity via Two Genetically Distinct Circuits. Neuron 102, 653–667.e6 (2019). [PubMed: 30879785]

23. Becker E & Kissileff H Inhibitory controls of feeding by the ventromedial hypothalamus. American Journal of Physiology-Legacy Content 226, 383–396 (1974).

24. Calarco CA et al. Molecular and cellular characterization of nicotinic acetylcholine receptor subtypes in the arcuate nucleus of the mouse hypothalamus. European Journal of Neuroscience 48, 1600–1619 (2018).

25. Page SJ, Zhu M & Appleyard SM Effects of acute and chronic nicotine on catecholamine neurons of the nucleus of the solitary tract. American Journal of Physiology-Regulatory, Integrative and Comparative Physiology 316, R38–R49 (2019). [PubMed: 30354182]

26. Huang H, Xu Y & van den Pol AN Nicotine excites hypothalamic arcuate anorexigenic proopiomelanocortin neurons and orexigenic neuropeptide Y neurons: similarities and differences. Journal of Neurophysiology 106, 1191–1202 (2011). [PubMed: 21653710]

27. Feng L, Sametsky EA, Gusev AG & Uteshev VV Responsiveness to nicotine of neurons of the caudal nucleus of the solitary tract correlates with the neuronal projection target. J Neurophysiol 108, 1884–1894 (2012). [PubMed: 22815399]

28. Mineur YS et al. Nicotine decreases food intake through activation of POMC neurons. Science 332, 1330–1332 (2011). [PubMed: 21659607]

29. Kallupi M, Xue S, Zhou B, Janda KD & George O An enzymatic approach reverses nicotine dependence, decreases compulsive-like intake, and prevents relapse. Sci Adv 4, eaat4751 (2018). [PubMed: 30345354]

30. Matta SG et al. Guidelines on nicotine dose selection for in vivo research. Psychopharmacology 190, 269–319 (2007). [PubMed: 16896961]

31. Paeger L. et al. Antagonistic modulation of NPY/AgRP and POMC neurons in the arcuate nucleus by noradrenalin. eLife 6,.

32. Holm S. A Simple Sequentially Rejective Multiple Test Procedure. Scandinavian Journal of Statistics 6, 65–70 (1979).

33. Baldwin PR, Alanis R & Salas R The Role of the Habenula in Nicotine Addiction. J Addict Res Ther Suppl 1, (2011).

34. Fowler CD, Lu Q, Johnson PM, Marks MJ & Kenny PJ Habenular α5* nicotinic receptor signaling controls nicotine intake. Nature 471, 597–601 (2011). [PubMed: 21278726]

35. Zuo W. et al. Nicotine regulates activity of lateral habenula neurons via presynaptic and postsynaptic mechanisms. Scientific Reports 6, 32937 (2016). [PubMed: 27596561]

36. Lee HW, Yang SH, Kim JY & Kim H The Role of the Medial Habenula Cholinergic System in Addiction and Emotion-Associated Behaviors. Frontiers in Psychiatry 10, (2019).

37. Arvin MC et al. Chronic Nicotine Exposure Alters the Neurophysiology of Habenulo-Interpeduncular Circuitry. J Neurosci 39, 4268–4281 (2019). [PubMed: 30867261]

38. Tuesta LM et al. GLP-1 acts on habenular avoidance circuits to control nicotine intake. Nature Neuroscience 20, 708–716 (2017). [PubMed: 28368384]

39. Duncan A. et al. Habenular TCF7L2 links nicotine addiction to diabetes. Nature 574, 372–377 (2019). [PubMed: 31619789]

40. Stamatakis AM et al. Lateral Hypothalamic Area Glutamatergic Neurons and Their Projections to the Lateral Habenula Regulate Feeding and Reward. J Neurosci 36, 302–311 (2016). [PubMed: 26758824]

41. Balthasar N. et al. Divergence of Melanocortin Pathways in the Control of Food Intake and Energy Expenditure. Cell 123, 493–505 (2005). [PubMed: 16269339]

42. Pei H, Sutton AK, Burnett KH, Fuller PM & Olson DP AVP neurons in the paraventricular nucleus of the hypothalamus regulate feeding. Molecular Metabolism 3, 209–215 (2014). [PubMed: 24634830]

43. Zhao R, Chen H & Sharp BM Nicotine-Induced Norepinephrine Release in Hypothalamic Paraventricular Nucleus and Amygdala Is Mediated by N-Methyl-d-aspartate Receptors and Nitric Oxide in the Nucleus Tractus Solitarius. J Pharmacol Exp Ther 320, 837–844 (2007). [PubMed: 17093131]

44. Hill J, Zoli M, Bourgeois J & Changeux J Immunocytochemical localization of a neuronal nicotinic receptor: the beta 2-subunit. J Neurosci 13, 1551–1568 (1993). [PubMed: 8463835]

45. Okuda H. et al. Immunocytochemical localization of nicotinic acetylcholine receptor in rat hypothalamus. Brain Research 625, 145–151 (1993). [PubMed: 8242393]

46. Chen J. et al. A Vagal-NTS Neural Pathway that Stimulates Feeding. Current Biology 30, 3986–3998.e5 (2020). [PubMed: 32822608]

47. Roman CW, Derkach VA & Palmiter RD Genetically and functionally defined NTS to PBN brain circuits mediating anorexia. Nat Commun 7, 11905 (2016). [PubMed: 27301688]

48. Campos CA, Bowen AJ, Schwartz MW & Palmiter RD Parabrachial CGRP Neurons Control Meal Termination. Cell Metabolism 23, 811–820 (2016). [PubMed: 27166945]

49. Essner RA et al. AgRP Neurons Can Increase Food Intake during Conditions of Appetite Suppression and Inhibit Anorexigenic Parabrachial Neurons. J Neurosci 37, 8678–8687 (2017). [PubMed: 28821663]

50. Wu Q, Boyle MP & Palmiter RD Loss of GABAergic Signaling by AgRP Neurons to the Parabrachial Nucleus Leads to Starvation. Cell 137, 1225–1234 (2009). [PubMed: 19563755]

51. Seppä T, Salminen O, Moed M & Ahtee L Induction of Fos-immunostaining by nicotine and nicotinic receptor antagonists in rat brain. Neuropharmacology 41, 486–495 (2001). [PubMed: 11543769]

52. Salminen O, Seppä T, Gäddnäs H & Ahtee L Effect of Acute Nicotine on Fos Protein Expression in Rat Brain During Chronic Nicotine and Its Withdrawal. Pharmacology Biochemistry and Behavior 66, 87–93 (2000). [PubMed: 10837847]

53. Sharp BM, Beyer HS, McAllen KM, Hart D & Matta SG Induction and Desensitization of the c-Fos mRNA Response to Nicotine in Rat Brain. Molecular and Cellular Neuroscience 4, 199–208 (1993). [PubMed: 19912923]

54. Dehkordi O. et al. Neuroanatomical Relationships between Orexin/Hypocretin-Containing Neurons/Nerve Fibers and Nicotine-Induced c-Fos-Activated Cells of the Reward-Addiction Neurocircuitry. J Alcohol Drug Depend 5, (2017).

55. Shankar K, Ramborger J, Bonnet-Zahedi S, Carrette LLG & George O Acute nicotine intake increases feeding behavior through decreasing glucagon signaling in dependent male and female rats. Hormones and Behavior 159, 105447 (2024). [PubMed: 37926623]

56. Kakava-Georgiadou N. et al. Considerations related to the use of short neuropeptide promoters in viral vectors targeting hypothalamic neurons. Sci Rep 9, 11146 (2019). [PubMed: 31366942]

57. Sapru HN Role of the hypothalamic arcuate nucleus in cardiovascular regulation. Auton Neurosci 175, 38–50 (2013). [PubMed: 23260431]

58. Bonnavion P, Mickelsen LE, Fujita A, de Lecea L & Jackson AC Hubs and spokes of the lateral hypothalamus: cell types, circuits and behaviour. J Physiol 594, 6443–6462 (2016). [PubMed: 27302606]

59. Fakhoury M, Salman I, Najjar W, Merhej G & Lawand N The Lateral Hypothalamus: An Uncharted Territory for Processing Peripheral Neurogenic Inflammation. Frontiers in Neuroscience 14, (2020).

60. Qin C, Li J & Tang K The Paraventricular Nucleus of the Hypothalamus: Development, Function, and Human Diseases. Endocrinology 159, 3458–3472 (2018). [PubMed: 30052854]

61. Khodai T & Luckman SM Ventromedial Nucleus of the Hypothalamus Neurons Under the Magnifying Glass. Endocrinology 162, bqab141 (2021). [PubMed: 34265067]

62. Tu L, Fukuda M, Tong Q & Xu Y The ventromedial hypothalamic nucleus: watchdog of whole-body glucose homeostasis. Cell & Bioscience 12, 71 (2022). [PubMed: 35619170]

63. Gray TS, Carney ME & Magnuson DJ Direct Projections from the Central Amygdaloid Nucleus to the Hypothalamic Paraventricular Nucleus: Possible Role in Stress-Induced Adrenocorticotropin Release. NEN 50, 433–446 (1989).

64. Chiang MC et al. Parabrachial Complex: A Hub for Pain and Aversion. J. Neurosci 39, 8225–8230 (2019). [PubMed: 31619491]

65. Sato M. et al. The lateral parabrachial nucleus is actively involved in the acquisition of fear memory in mice. Molecular Brain 8, 22 (2015). [PubMed: 25888401]

66. Arai K. et al. Nicotine infusion alters leptin and uncoupling protein 1 mRNA expression in adipose tissues of rats. American Journal of Physiology-Endocrinology and Metabolism 280, E867–E876 (2001). [PubMed: 11350768]

67. Simpson S, Shankar K, Kimbrough A & George O Role of Corticotropin-Releasing Factor in Alcohol and Nicotine Addiction. Brain Res 1740, 146850 (2020). [PubMed: 32330519]

68. Jaehne A, Loessl B, Bárkai Z, Riemann D & Hornyak M Effects of nicotine on sleep during consumption, withdrawal and replacement therapy. Sleep Medicine Reviews 13, 363–377 (2009). [PubMed: 19345124]

69. Stojakovic A, Espinosa EP, Farhad OT & Lutfy K Effects of nicotine on homeostatic and hedonic components of food intake. J Endocrinol 235, R13–R31 (2017). [PubMed: 28814527]

70. van der Kooy D, Koda LY, McGinty JF, Gerfen CR & Bloom FE The organization of projections from the cortes, amygdala, and hypothalamus to the nucleus of the solitary tract in rat. Journal of Comparative Neurology 224, 1–24 (1984). [PubMed: 6715573]

71. Schilström B, Svensson HM, Svensson TH & Nomikos GG Nicotine and food induced dopamine release in the nucleus accumbens of the rat: Putative role of α7 nicotinic receptors in the ventral tegmental area. Neuroscience 85, 1005–1009 (1998). [PubMed: 9681941]

72. Wheeler AL, Wessa M, Senzai Y, Krishnan V, Maeno H, Dong Y, et al. Functional connectomics of fear conditioning in mice. Nature Neuroscience. 2013;16: 494–503.

73. Vetere G, Restivo L, Cole CJ, Ross PJ, Ammassari-Teule M, Josselyn SA, et al. A connectivity map of fear memory retrieval in the hippocampal-prefrontal circuit. Nature Neuroscience. 2017;20: 364–372.

74. Kimbrough A, Cole M, Manders T, George O. Functional connectivity associated with nicotine addiction: A network perspective. Journal of Neuroscience Research. 2020;98: 1357–1375.

75. Kimbrough A, et al. Revisiting the cholinergic system and its role in addiction. Addiction Biology. 2021;26: e12908. [PubMed: 32329567]

76. Carrette LLG, Manders T, Bonnet-Zahedi S, George O. Addiction-related neuroplasticity visualized through connectomics: Habenula and amygdala networks. Neuropharmacology. 2023;206: 108865.

77. Carrette LLG, et al. Functional mapping of the hypothalamus in substance use disorder. Brain Research. 2023;1801: 148306.

78. Roland R, Shankar K, et al. Nicotine dependency and altered functional connectivity: Implications for therapeutic intervention. Frontiers in Neural Circuits. 2023;17: 2128.

79. Stamatakis AM, Van Swieten M, Schwarz LA, et al. Lateral hypothalamic area glutamatergic neurons and their projections to the lateral habenula regulate feeding and reward. Journal of Neuroscience. 2016;36: 302–311. [PubMed: 26758824]
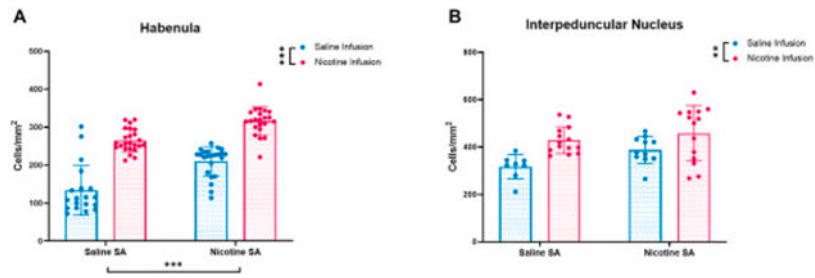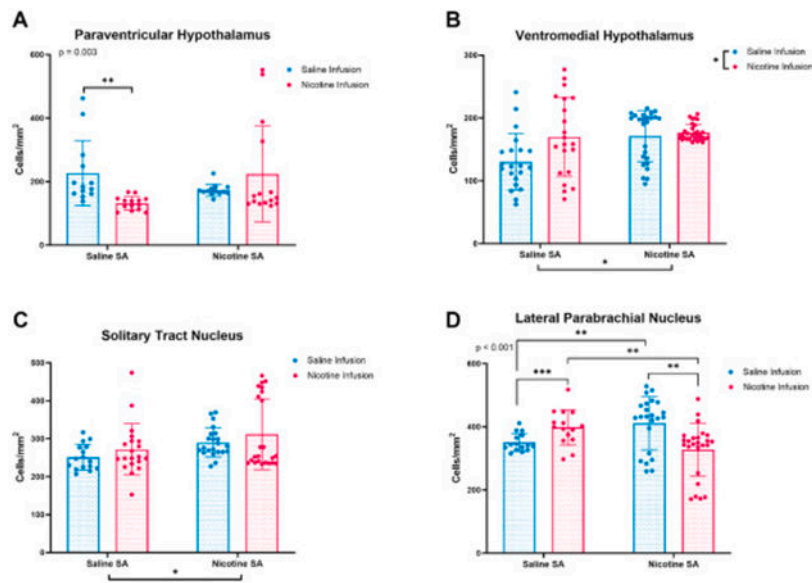
Figure 1. Effect of nicotine self-administration and acute nicotine infusion on the habenular-IPN axis.

A) Average FOS activation in the habenula between Sal/Sal, Sal/Nic, Nic/Sal, and Nic/Nic treatment groups. SA $p < 0.001$, infusion $p < 0.001$ (linear mixed model). N = 19-24 slices per treatment group. B) Average FOS activation in the interpeduncular nucleus between Sal/Sal, Sal/Nic, Nic/Sal, and Nic/Nic treatment groups. Infusion $p = 0.002$ (linear mixed model). N = 8-14 slices per treatment group. Blue bars represent acute infusion of 0.9% saline. Red bars represent acute infusion of 0.09 mg/kg nicotine. **$p < 0.01$, ***$p < 0.001$.
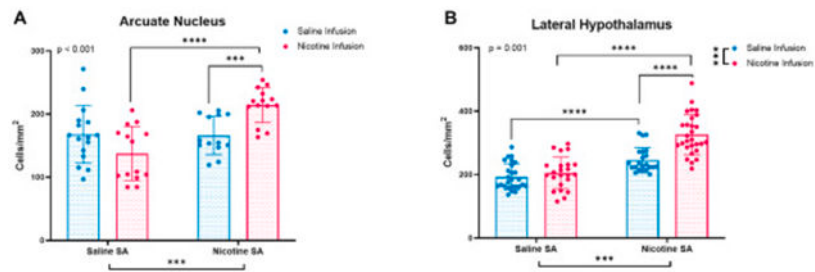
Figure 2. Effect of nicotine self-administration and acute nicotine infusion on the arcuate nucleus and lateral hypothalamus.

A) Average FOS activation in the arcuate nucleus between Sal/Sal, Sal/Nic, Nic/Sal, and Nic/Nic treatment groups. SA × infusion interaction $p < 0.001$, SA $p < 0.001$ (linear mixed model). N = 13-16 slices per treatment group. B) Average FOS activation in the lateral hypothalamus between Sal/Sal, Sal/Nic, Nic/Sal, and Nic/Nic treatment groups. SA × infusion interaction $p = 0.001$, SA $p < 0.001$, infusion $p < 0.001$ (linear mixed model). N = 22-28 slices per treatment group. Blue bars represent acute infusion of 0.9% saline. Red bars represent acute infusion of 0.09 mg/kg nicotine. $**p < 0.01$, $***p < 0.001$, $***p < 0.001$.

Figure 3. Effect of nicotine self-administration and acute nicotine infusion on anorexigenic centers in the hypothalamus and hindbrain.

A) Average FOS activation in the paraventricular nucleus between Sal/Sal, Sal/Nic, Nic/Sal, and Nic/Nic treatment groups. SA x infusion interaction $p = 0.003$ (linear mixed model). N = 13-15 slices per treatment group. B) Average FOS activation in the ventromedial hypothalamus between Sal/Sal, Sal/Nic, Nic/Sal, and Nic/Nic treatment groups. SA $p = 0.018$, infusion $p = 0.024$ (linear mixed model). N = 21-30 slices per treatment group. C) Average FOS activation in the nucleus of the solitary tract between Sal/Sal, Sal/Nic, Nic/Sal, and Nic/Nic treatment groups. SA $p = 0.048$ (linear mixed model). N = 16-23 slices per treatment group. D) Average FOS activation in the lateral parabrachial nucleus between Sal/Sal, Sal/Nic, Nic/Sal, and Nic/Nic treatment groups. SA x infusion interaction $p < 0.001$ (linear mixed model). N = 15-26 slices per treatment group. Blue bars represent acute infusion of 0.9% saline. Red bars represent acute infusion of 0.09 mg/kg nicotine. *$p < 0.05$, **$p < 0.01$, ***$p < 0.001$.
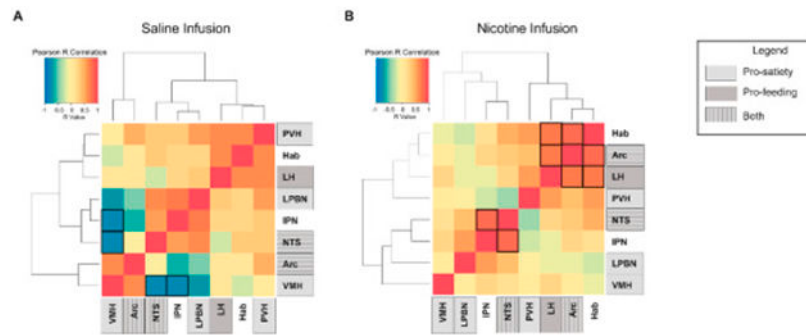
Figure 4. Heatmap representation of correlation in FOS activation between brain regions.
A) Correlations following acute injection of saline (N = 8). B) Correlations following acute injection of nicotine (N = 10). Color key represents Pearson R values, and significant correlations (p < 0.05) are highlighted by black boxes. Abbreviations: arcuate (Arc), habenula (Hab), interpeduncular nucleus (IPN), lateral hypothalamus (LH), lateral parabrachial nucleus (LPBN), paraventricular hypothalamus (PVH), nucleus of the solitary tract (NTS), ventromedial hypothalamus (VMH). Names in light gray background designate pro-satiety regions, names in dark grey background designate pro-feeding regions, names in striped background designate regions that have both pro-feeding and pro-satiety actions.
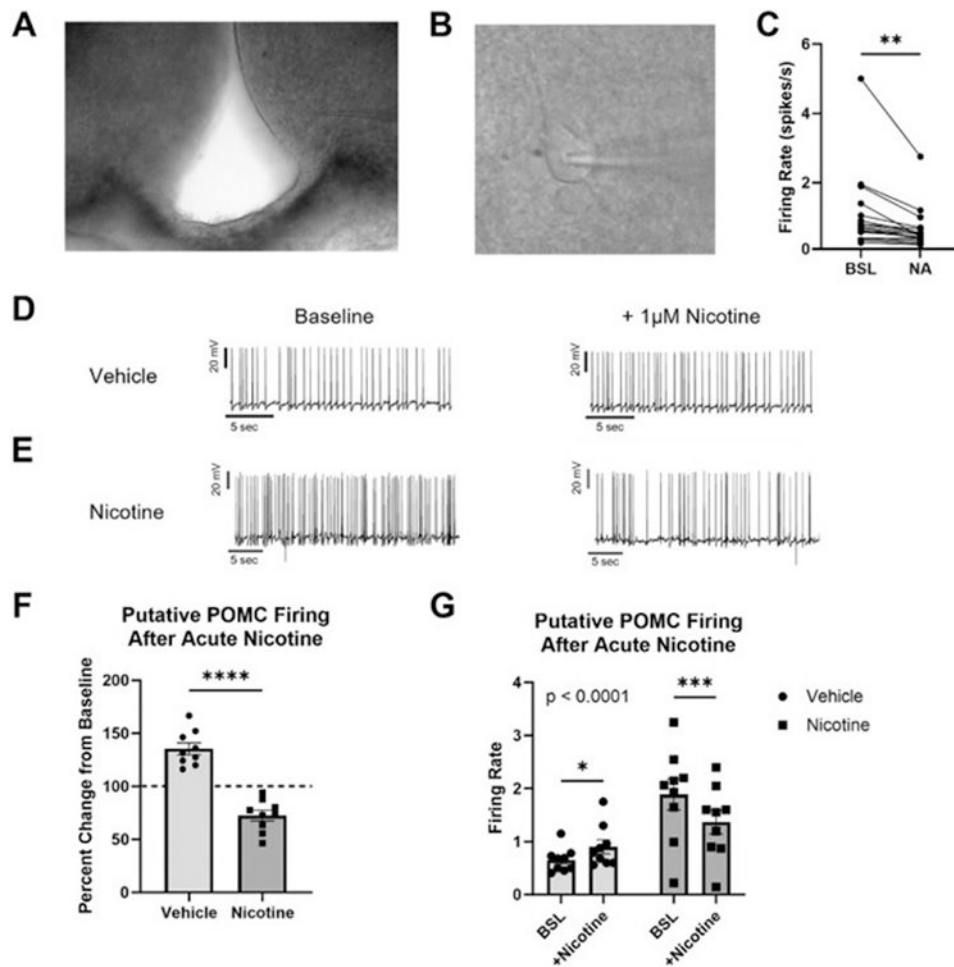
Figure 5. Effect of chronic nicotine and acute nicotine application on POMC neuron activity.
A) Representative image of the arcuate nucleus region used for recording. B) Representative image of whole-cell patch of putative POMC neuron. C) Firing rate of neurons before and after application of 10 μM noradrenaline. D) Representative image of spike recording at baseline (left) and following application of 1 μM nicotine (right) in vehicle animals. E) Representative image of spike recording at baseline (left) and following application of 1 μM nicotine (right) in nicotine animals. F) Average percent change of firing rate from baseline in vehicle (light gray) and nicotine (dark gray) cells following 1 μM nicotine application. p = 0.0003 (Student's t-test). Data are expressed as number of cells recorded per treatment group. G) Average firing rate of POMC cells from vehicle (light gray) and nicotine (dark gray) at baseline and after 1 μM nicotine application. Chronic nicotine x treatment interaction p = 0.00009 (two-way ANOVA). *p < 0.05 (Sidak's multiple comparisons post hoc test). Vehicle N = 9, nicotine N = 9.